Available online at www.sciencedirect.com
ScienceDirect
Nuclear Physics B Proceedings Supplement 00 (2012) 1–4
Nuclear Physics B Proceedings Supplement

Status and prospects of J-PARC KOTO experiment

E. Iwai for the KOTO Collaboration

Department of Physics, Osaka University, Toyonaka, Osaka, 560-0043, Japan

Abstract

The J-PARC KOTO experiment was designed to observe the rare decay of long lived neutral kaons, $K_L \to \pi^0\nu\bar{\nu}$. The goal of KOTO is to observe the decay with the sensitivity of the Standard Model prediction, and search for New Physics beyond the Standard Model. The KOTO apparatus consists of a high intensity K_L beam line, an electromagnetic calorimeter, and veto counters. The beam line and the calorimeter have already been built at J-PARC, and the veto counters are being constructed and tested for the coming and physics runs. In this paper, the KOTO experiment will be briefly introduced and the status and the prospects of the KOTO experiment will be described.

Keywords: New Physics, Kaon, $K_L \to \pi^0\nu\bar{\nu}$, CP violation, KOTO experiment, BEACH 2012, proceedings

1. Introduction

The KOTO experiment aims to observe a rare decay of long lived neutral kaons, $K_L \to \pi^0\nu\bar{\nu}$. By observing the decay, we can search for New Physics beyond the Standard Model (SM).

1.1. Physics

In the SM, the decay process is mediated by the second order diagrams of the electroweak interactions with the flavor-changing neutral current process within three generations in the quark sector: $s \to t \to d$. The branching ratio of the $K_L \to \pi^0\nu\bar{\nu}$ decay is proportional to η^2 where η represents an imaginary part of the Cabibbo-Kobayashi-Maskawa (CKM) matrix elements in Wolfenstein's parametrization[1], which causes CP violation. The feature of this decay mode is that its theoretical error on calculation is only 2 %. The branching ratio of the $K_L \to \pi^0\nu\bar{\nu}$ decay is predicted to be $Br_{\rm SM}(K_L \to \pi^0\nu\bar{\nu}) = (2.43^{+0.40}_{-0.37} \pm 0.06) \times 10^{-11}$[2], and the uncertainty is dominated by the currently measured CKM parameters.

If a non-SM particle propagates in the loop, the branching ratio of the $K_L \to \pi^0\nu\bar{\nu}$ decay may be different from the SM prediction. Because the decay directly violates the CP symmetry, the deviation of the branching ratio from the SM prediction also implies new sources of the CP violation. There are some theoretical models of New Physics beyond the SM which enhance the branching ratio of the decay.

The upper limit of the branching ratio of the decay was set by KEK-PS E391a experiment, a pilot experiment of the KOTO experiment, to be 2.6×10^{-8} (90 % C.L.)[3, 4]. There is another upper limit indirectly set by $K^+ \to \pi^+\nu\bar{\nu}$ isospin rotation, called Grossman-Nir bound[5], and to be 1.4×10^{-9} (90 % C.L., by E787/E949 result[6]), about 2 orders of magnitude larger than the SM prediction. KOTO will explore the remaining room between the Grossman-Nir bound and the SM prediction, and to search for New Physics.

1.2. Experimental method

A decay volume for K_L is surrounded by particle detectors. The signature of a $K_L \to \pi^0\nu\bar{\nu}$ decay is that there are two photons from a π^0 decay and no other visible particles in the final state. An electromagnetic calorimeter is placed downstream of the decay volume to detect the two photons. All the K_L decay modes except $K_L \to \pi^0\nu\bar{\nu}$ and $K_L \to \gamma\gamma$ have at least two charged particles, or two or more extra photons in the final state.

These decays can be rejected by detecting additional particles with the surrounding detectors. The $K_L \to \gamma\gamma$ decays can be rejected by requiring a finite transverse momentum for the two photon system. In case of the $K_L \to \pi^0\nu\bar{\nu}$ decay, the two photon system has a finite transverse momentum, because the undetected two neutrinos take some momentum away. We calculate the decay vertex and reconstruct the $K_L \to \pi^0\nu\bar{\nu}$ decay from two photons in the calorimeter with the assumption that the two photons come from a π^0 decay on the z-axis.

2. Apparatus and its status

Figure 1 shows a side view of the KOTO detector. We reuse the E391a detector with a number of upgrades. The apparatus of KOTO experiment is characterized by a high intensity K_L beam, a CsI calorimeter, veto detectors and a waveform digitization. In this section, we describe the apparatus and its status.

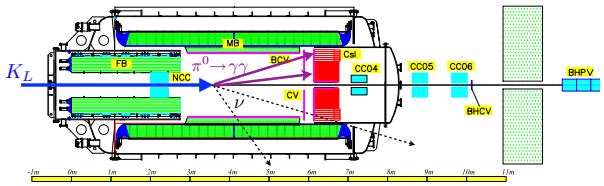

Figure 1: Side view of the KOTO detector. The decay volume in the middle of the detector is surrounded by hermetic particle detectors.

2.1. K_L beam line

Figure 2 shows an overview of the beam line. The J-PARC main ring was designed to deliver 30 GeV protons to our experimental hall for 0.7 seconds in every 3.3 seconds. The K_L particles are produced by the primary protons striking a common target, and the K_L particles are transported through a neutral beam line to the KOTO detector. The target consists of five Ni disks with the total thickness of 53.9 mm. The neutral beam line is located at 16° from the primary proton beam in a horizontal plane. The beam line is 21 m long and consists of a pair of collimators, a sweeping magnet, and a γ absorber. The first collimator is 400 cm long, and the second collimator is 500 cm long. They are made of iron except for the 50 cm long region at the upstream end, which are made of tungsten. The magnet is placed between the two collimators to sweep out charged particles. The γ absorber is made of 7-cm-long lead.

The beam line construction was completed in 2009. We aligned the collimating system and measured the beam profile with the scintillating fiber hodoscope[7] in 2010 and 2011.

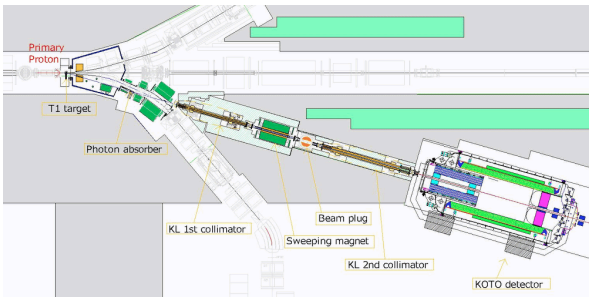

Figure 2: Schematic view of the neutral beam line.

We also measured the number of K_Ls produced per protons on target and their momenta. We detected two charged particles and two photons with hodoscopes and calorimeters, and reconstructed them by assuming that they were from $K_L \to \pi^+\pi^-\pi^0$ decay. Figure 3 shows the invariant mass distribution and momentum spectra of reconstructed K_Ls at the exit of the beam line[8]. The measured K_L yield was 2.6 times higher that what was assumed in the proposal.

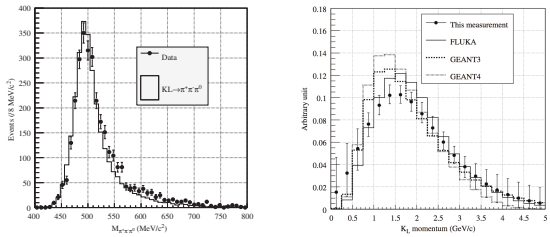

Figure 3: The observed invariant mass distribution (left) and momentum spectra at the exit of the beam line (right) of reconstructed K_Ls[8].

2.2. CsI calorimeter

The CsI electromagnetic calorimeter is placed downstream of the decay volume, as shown in Fig. 1, to measure energies, timings and incident positions of photons. To improve granularity and get more shower shape information of photons, 496 pieces of the E391a crystals with the dimension of $7 \times 7 \times 30$ cm^3 were replaced by 2240 crystals with the dimension of $2.5 \times 2.5 \times 50$ cm^3 and 476 crystals with the dimension of $5 \times 5 \times 50$ cm^3. Those are undoped CsI crystals used at the Fermilab KTeV experiment.

We first measured the energy, timing, and position resolutions of a small calorimeter consisting of 144 2.5

cm square crystals with positrons. Figure 4 shows the obtained energy and timing resolutions[9]. We understood the performance from the first principles. We then stacked crystals and built the calorimeter at J-PARC in 2010. The calorimeter was tested with cosmic ray muons, $K_L \to \pi^0\pi^0\pi^0$ and $K_L \to \pi e \nu$ decays. Figure 5 shows an event display of the calorimeter and invariant mass distribution of 6 photon events. We confirmed and established the calibration method of the calorimeter.

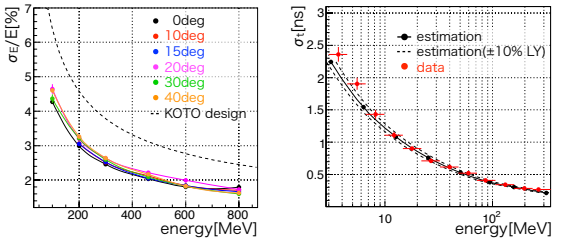

Figure 4: Observed energy and timing resolutions of the small calorimeter[9]. left) Energy resolutions for various energies and incident angles. The dashed lines show the designed value of the KOTO experiment. right) Timing resolutions as a function of the deposit energy in a crystal. The black solid line with dots shows the estimated timing resolution and the red dots show the result obtained with data.

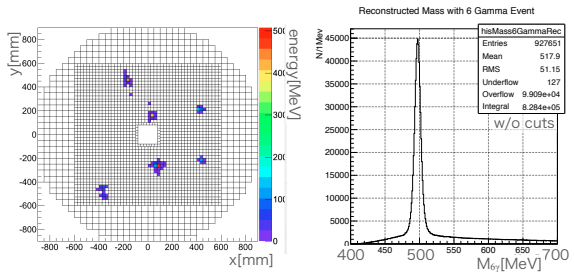

Figure 5: Event display of the CsI calorimeter and the invariant mass distribution of 6 photon events.

2.3. Veto detectors

Veto detectors surround the decay volume, as shown in Fig. 1, to detect the additional particles except two photons from π^0 decays. Most of the veto detectors are upgraded.

One of the upgraded veto detectors is Charged Veto (CV). The CV is placed in front of the CsI calorimeter to detect charged particles hitting the calorimeter. It consists of two layers. One of them is placed on the upstream surface of the calorimeter, and the other is placed 25 cm upstream of the calorimeter. Each layer consists of thin (3 mm) plastic-scintillators to suppress neutron interaction. Signals from the scintillators are read by MPPC through WLS fibers. To achieve a small detection inefficiency, light yield is crucial. We built two layers of CV and measured the light yield of them at the K_L beam line. The measured light yields were large enough to achieve the small detection inefficiency.

Neutron Color Counter (NCC) is another upgraded detector. The NCC consists of 48 modules made of 3 CsI blocks glued together, and is placed at the entrance of the decay volume surrounding the K_L beam. The NCC is designed not only to detect photons from K_L decays, but also to measure the flux and energy spectrum of beam halo neutrons. All the NCC modules were constructed, and confirmed to have large enough light yields with cosmic ray test.

Beam Hole Photon Veto is also an upgraded detector. The BHPV is placed at the downstream end of our detector system to detect photons escaping from the decay volume through the beam hole in the calorimeter. The BHPV consists of 25 Cerenkov counter modules. Each module is composed of a lead plate, a stack of aerogel tiles, a mirror, a Winston cone, and a PMT. The lead plate converts photons to electrons and positrons, and the aerogel tiles emit Cerenkov light from the electrons and positrons. By using Cerenkov light, BHPV is not sensitive to heavy particles such as neutrons in the beam core. To suppress shower components going back to other veto counters, BHPV is placed inside a radiation shield.

Main Barrel (MB) surrounds the side of the decay volume. The MB consists of 32 modules, and each module consists of an existing module from the E391a experiment[10] and a new additional module. The E391a module is made of 45 layers of lead and plastic-scintillator sheets, and its total thickness is 14 X_0. We plan to add 5 X_0 thick modules inside the existing modules. The designing of the additional modules is finished and a prototype module is being prepared. By adding the new modules inside the existing modules, the number of $K_L \to \pi^0\pi^0$ background caused by the detection inefficiency of the MB, which is the largest background, is estimated to be suppressed by a factor of 7.

2.4. Waveform digitization and data acquisition

Signals from all the detectors are read out by Flash ADC (FADC) boards. At the beginning, signals from all the detectors are digitized by 14-bit 125 MHz FADCs with 10-pole Bessel filter. As the beam power increases, 125 MHz FADCs for some detectors, such as detectors in the beam core, will be replaced to 12-bit 500

MHz FADCs without the filter, to cope with the higher counting rate. The 125 MHz FADC boards were already manufactured, and operated for the calorimeter and veto detectors. For the 500 MHz FADC board, prototype boards were produced and tested. We are ready to manufacture the 500 MHz FADC boards.

Figure 6 shows an overview of the DAQ system. Digitized waveform data is stored in the boards temporally for 4 μs. Each FADC board receives analog inputs, calculates local sum of them and sends the sum to one of Level1(L1) trigger boards every 8 ns. A master control board of this DAQ system called MACTRIS communicates with the L1 trigger boards, generates L1 triggers based on those sums, and sends triggers to the FANOUT boards. The FANOUT boards fan-out the triggers and also clock signals to each FADC board. When a FADC board receives a trigger, the board sends corresponding waveform data to a so called Level2(L2) trigger board. The L2 trigger board has dual memories on it, and keeps storing data sent from the FADC boards during a spill after some event selections. The stored data is sent to an event building system during the next spill.

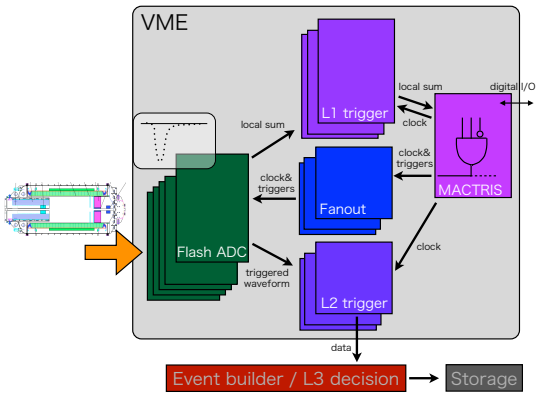

Figure 6: Overview of the DAQ system for KOTO experiment.

Reading out data through the above scheme was tested and established, with relatively simple L1 selection and no L2/L3 selections. We will keep developing and implementing more sophisticated selection algorithms in the trigger system.

3. Prospects

We will have the first physics runs in 2013 spring. The experimental sensitivity will cross the Grossman-Nir bound and New Physics search will be started. After the first physics runs, a beam shut-down is planned for linuc upgrade. With the linuc upgrade, we expect to have more beam power. The expected final sensitivity of KOTO experiment will reach the SM prediction, and KOTO will explore extensive parameter spaces of theories which give the branching ratio of $K_L \to \pi^0\nu\bar{\nu}$ above the SM prediction.

4. Summary

The KOTO experiment is the experiment to search for New Physics by observing the $K_L \to \pi^0\nu\bar{\nu}$ decay. Experimental apparatus is almost ready to take physics data, and the first physics run will start in 2013 spring. We will soon begin New Physics search and the experimental sensitivity will cross the Grossman-Nir bound with the first physics run, and will reach the SM prediction at the end.

References

[1] L. Wolfenstein, Phys. Rev. Lett. **51**, 1945 (1983).
[2] J. Brod, M. Gorbahn, and E. Stamou, Phys. Rev. D **83**, 034030 (2011).
[3] J. K. Ahn *et al.* (E391a Collaboration), Phys. Rev. D **81**, 072004 (2010).
[4] H. Morii, *Experimental Study of the Decay* $K_L^0 \to \pi^0\nu\bar{\nu}$, PhD thesis, Kyoto University, (2010).
[5] Y. Grossman and Y. Nir, Phys. Lett. B **398**, 163 (1997).
[6] A. V. Artamonov *et al.*, Phys. Rev. Lett. **101**, 191802 (2008).
[7] G. Takahashi *et al.*, Jpn. J. Appl. Phys. **50**, 036701 (2011).
[8] K. Shiomi *et al.*, Nucl. Instrum. Meth. A **664**, 264 (2012).
[9] E. Iwai, *CsI calorimeter for the J-PARC KOTO experiment*, PhD thesis, Osaka University, (2012).
[10] Y. Tajima *et al.*, Nucl. Instrum. Meth. A **592**, 261 (2008).